Characterization of a Functional C3A Liver Spheroid Model

Harriet Gaskella,b, Parveen Sharmaa, Helen E Colleyc, Craig Murdochc, Jean G Sathishd, Daniel J Antoinea, Dominic P Williamsb, Steven D Webba,e.

More predictive in vitro liver models are a critical requirement for preclinical screening of compounds demonstrating hepatotoxic liability. 3D liver spheroids have been shown to have an enhanced functional lifespan compared to 2D monocultures; however a detailed characterisation of spatiotemporal function and structure of spheroids still needs further attention. We have developed and characterized the structure and function of a 3D liver spheroid model formed from C3A hepatoma cells. Spheroids maintained a compact *in vivo*-like structure with zonation features and with no necrotic core, for up to 32 days. MRP2 and Pgp transporters had polarised expression on the canalicular membrane of cells in the spheroids, with MRP2 able to functionally transport CMFDA substrate into these canalicular structures. Spheroids were able to synthesise and secrete albumin and urea as well as expressing CYP2E1. Penetration of doxorubicin throughout the spheroid core was also demonstrated. Dose-dependent toxicity occurred in response to model hepatotoxins, with spheroids showing increased susceptibility to diclofenac than 2D monolayer cultures, with an IC50 of 270 µM and 370 µM respectively. We therefore developed an alternative method for creating C3A liver spheroids and demonstrated cellular polarisation and zonation, liver-specific functionality and toxicological response, confirming a more *in vivo*-like liver model when compared to standard 2D liver models.

Introduction

Drug-induced liver injury (DILI) is a common side-effect of many therapeutic compounds that often results in the failure of compounds in discovery and development resulting in compounds not reaching the market, or being withdrawn (Lazarou et al. 1998). Exposure to hepatotoxic compounds can result in liver failure, a life threatening condition, usually requiring a liver transplant (Norris et al. 2008; Reuben et al. 2010). Predictive *in vitro* liver models are essential during initial drug screening in order to conduct an accurate risk assessment leading to better candidate selection early in the drug discovery and development process. Commonly used *in vitro* models to detect liver injury include freshly isolated human hepatocytes cultured as a monolayer, suspension or sandwich culture (Godoy et al. 2013). However the rapid decline in function and viability of these cells *ex vivo* and inter-donor variability are a major limitation to their use (Donato et al. 2008; Gomez-Lechon et al. 2004; Khetani et al. 2015; LeCluyse et al. 2005). Immortalised hepatocarcinoma cell lines, such as HepG2, C3A, Huh7 and HepaRG, have been used as an alternative to freshly isolated hepatocytes since they have extended lifespans and their clonal nature reduces inter-experimental variability (Donato et al. 2008; LeCluyse et al. 2012). However when cultured as a 2D monolayer these cell lines demonstrate low functionality and an altered phenotype compared to human hepatocytes *in vivo* (Godoy et al. 2013; Guo et al. 2011; LeCluyse et al. 2012).

A second disadvantage of commonly used *in vitro* models is a lack of 3D structure, which has a significant effect on the hepatocyte morphology, function, phenotype, signalling and toxicological

response (Gomez-Lechon et al. 1998; Semler et al. 2000; Wells 2008). A simple, high-throughput method of culturing cells in 3D is by creating spheroids. Spheroids, also known as microtissues or organoids, are spherical 3D clusters of cells with direct cell-cell contacts that can be formed using a variety of techniques with or without the use of scaffolds (Friedrich et al. 2009; Godoy et al. 2013; van Zijl and Mikulits 2010; Wong et al. 2011). Additionally, spheroids have the potential to be used for long-term repeat dose studies as well as being amenable to high-throughput assays, an advantage for drug screening (Friedrich et al. 2009; Wong et al. 2011). Unlike more complicated 3D cell culture techniques, such as perfused cultures, bioreactors, scaffold or chip-based systems, spheroids are simple to generate, inexpensive to culture, reproducible and easy to analyse (Godoy et al. 2013). The use of spheroids as a model for screening of hepatotoxins is fairly novel; however in other areas of research spheroids are a well-established 3D cell culture technique. Preliminary research into liver spheroids has shown some promising results. Isolated human hepatocytes survive and are functional in spheroids for up to 4 weeks, sustaining Phase 1 and 2 enzyme expression, albumin and urea synthesis and expression of liver-specific markers. Additionally bile canaliculi structures form in the spheroids, indicating polarisation of hepatocytes and *in vivo*-like morphology and phenotype (Tostoes et al. 2012). Additionally, when cultured in spheroids, hepatocytes show cuboidal morphology, enhanced cell-cell contacts, polarisation and production of extracellular matrix (ECM) components (Peshwa et al. 1996; Wong et al. 2011).

Multiple studies have also shown that hepatocarcinoma cell lines when cultured in spheroids have enhanced function when compared to monolayer cultures, overcoming the main disadvantages seen with these cells in 2D culture. HepaRG cells have been cultured as spheroids and show a significant improvement in albumin and AboB production, increases in liver specific gene expression and activity, and induction of CYP enzymes when compared to 2D cultured cells (Takahashi et al. 2015; Wang et al. 2015). Spheroids created from Huh7 cells display expression of phase I and II enzymes as well as polarisation of various receptors (Sainz et al. 2009). HepG2 cell spheroids have been shown to be viable and functional for at least 28 days, determined by increased albumin production, increased expression of liver specific enzymes and activity of Phase I and II enzymes, increased sensitivity to hepatotoxins, bile canaliculi formation and transporter function (Ramaiahgari et al. 2014). In addition to this, spheroids formed from HepG2 cells show over-expression of genes involved in xenobiotic and lipid metabolism (Chang and Hughes-Fulford 2009; Ramaiahgari et al. 2014; Sainz et al. 2009; Takahashi et al. 2015; Tostoes et al. 2012; Wang et al. 2015). This increase in liver-specific function has been shown to raise the sensitivity of HepG2 cells to hepatotoxic compounds and allows for more realistic repeat dosing strategies (Ramaiahgari et al. 2014). C3A cells are a subclone of HepG2 cells with some advantages, selected for their strong contact-inhibited growth characteristics, as well as high-albumin production, alpha fetoprotein and transferrin synthesis and are able to grow in glucose deficient media (Nibourg et al. 2012). This cell line may therefore have advantages over others when cultured in spheroids, with a reduced proliferation rate, more representative of the *in vivo* situation (Wrzesinski et al. 2013). Previous studies of C3A spheroids have revealed superior function over 2D cultures, however further investigation into the canalicular structures, zonation, liver-specific

functionality and toxicological response of this model is necessary before widespread use for drug screening (Fey and Wrzesinski 2012; Wrzesinski and Fey 2013; Wrzesinski et al. 2013).

3D liver spheroids show promise through enhanced functionality compared to 2D cultures, and could provide a valuable tool for investigating hepatotoxic drugs in pre-clinical safety testing. However, despite the increasing interest and use of 3D liver models, little research has gone into validating key structural and functional parameters such as spheroid size, internal structure, oxygen and nutrient diffusion, drug penetration, cellular polarisation and liver-specific functionality (Asthana and Kisaalita 2012; Curcio et al. 2007; Olive et al. 1992). In this study we developed and optimised a liver spheroid model using C3A hepatocarcinoma cells and characterised their spatiotemporal structure and function providing essential optimising parameters and an invaluable tool for investigating acute and chronic liver injury.

Experimental

Agarose type V high gelling temperature (A3768), agarose low electroendosmosis (EEO) (A9539), fetal bovine serum (FBS) , penicillin-streptomycin, 1 x phosphate buffered saline (PBS), paraformaldehyde (PFA), Triton X-100, Tween20, Tris, bovine serum albumin (BSA), DMSO, doxorubicin, Paracetamol and diclofenac were purchased from Sigma Aldrich, Missouri, USA. C3A cells and Eagle's minimal essential medium (EMEM) were purchased from LGC standards, Middlesex, UK. Ultra-Low Adherence (ULA) plates were purchased from Corning, NY, USA. Cell Titer-Glo assay was purchased from Promega, Madison, USA. Albumin Human ELISA Kit (ab108788), Urea Assay Kit (ab83362), MRP2 (ab3373) and Pgp (ab8189) antibodies were purchased from Abcam, Cambridge, UK. Prolong Gold (P36930), hoechst (H3570), Alexa Fluor 568 Phalloidin (A12380) and Cell Tracker (CMFDA) (C7025) were purchased from Life Technologies, Carlsbad, CA, USA. Alexa Fluor 488 Donkey Anti-Mouse (R37114) was purchased from Invitrogen, Carlsbad, CA, USA.

Spheroid formation and growth

C3A cells were maintained in EMEM supplemented with 10 % FBS and 1 % penicillin-streptomycin under standard cell culture conditions. For 2D monolayer experiments C3A cells were seeded and left to adhere for 24 hours and confirmed to be 100 % confluent before analyses.

Spheroids were created using the liquid overlay technique as previously described (Yuhas et al. 1977). Briefly, 100 µl of sterile 1.5 % Agarose (high gelling temperature) in EMEM was added per well to flat-bottomed 96-well cell culture plates to form a low-adherence surface. Additionally ULA plates were used as a comparison. C3A cells were seeded at 500, 750, 1000, 1500, 2000 or 2500 cells/well in 100 µl media and left for 72 hours to form spheroids. Media was renewed twice weekly and spheroids were cultured for up to 32 days. Images of spheroids in culture were taken by phase-contrast microscopy through 4 X objective and spheroid diameter measured from these.

Histological analysis

Spheroids were washed in PBS, fixed for 1 hour in 4 % PFA and embedded in 2 % Agarose (low EEO) in 4 % PFA then paraffin embedded. Tissue sections were cut and stained with haematoxylin and eosin (H&E) or as previously described (Colley et al. 2011). Immunohistochemistry for Ki-67, carbamoyl-phosphate synthase 1 (CPS1) and CYP2E1 was carried out by the Department of Veterinary Pathology, Leahurst Campus, University of Liverpool, UK.

Immunofluorescence analysis of spheroids

Spheroids were transferred to ULA plates, washed three times in PBS and fixed with 4 % PFA for 1 hour at 4 °C. Spheroids were washed again then permeabilized with 0.5 % Triton X-100 in Tris-Buffered Saline with 0.05 % Tween20 (TBST) overnight at 4 °C and then blocked with 0.1 % Triton X-100/3% BSA in TBST for 2 hours at room temperature (RT). Primary antibodies Multidrug resistance protein-2 (MRP2) and P-glycoprotein (Pgp) were diluted 1:20 in 0.1 % Triton X-100 /1 % BSA in TBST were incubated with the spheroids overnight at 4 °C. Spheroids underwent three 1 hour washes with 1 % Triton X-100 in TBST then incubated with secondary Alexa Fluor 488 Donkey Anti-Mouse antibody diluted 1:1000, Hoechst diluted 1:5000 and Phalloidin diluted 1:250 in 0.1 % Triton X-100 /1 % BSA in TBST overnight at 4 °C. Spheroids were finally washed for 1 hour then mounted with Prolong Gold onto a glass microscope slide. Maximum intensity projection images of spheroids were taken on Zeiss microscope using 40 X oil objective.

Immunofluorescence analysis of 2D monolayers

Cells were washed in PBS for 30 min at 4 °C then fixed with 2 % PFA for 30 min at 4 °C. Cells were permeabilized with two 15 min washes in 0.2 % Tween-20/ 0.5 % Triton X-100 in PBS at 4 °C and blocked for 30 min in 5 % BSA/ 0.2 % Tween-20/ 0.5 % Triton X-100 in PBS at room temperature. Primary antibodies Multidrug resistance protein-2 (MRP2) and P-glycoprotein (Pgp) were diluted in 5 % BSA/ 0.2 % Tween-20/ 0.5 % Triton X-100 in PBS and incubated with cells overnight at 4 °C. Cells underwent three 15 min washes in 0.2 % Tween-20/ 0.5 % Triton X-100 in PBS then incubated with secondary Alexa Fluor 488 Donkey Anti-Mouse antibody diluted 1:1000, Hoechst diluted 1:5000 and Phalloidin diluted 1:250 in 5 % BSA/ 0.2 % Tween-20/ 0.5 % Triton X-100 in PBS for 1 hour at room temperature. Cells underwent three 15 min washes in PBS then were mounted with Prolong gold onto a glass microscope slide. Images were taken on Zeiss microscope using 40 X oil objective.

Analysis of transporter function

Spheroids and monolayers were incubated with 5 µM 5-chloromethylfluorescein diacetate (CMFDA) in EMEM for 30 min at 37 °C. CMFDA is membrane permeable until it enters cell and is converted to glutathione-methylfluorescein (GSMF), a cell impermeable substrate for MRP2. Cells and spheroids were washed in PBS and prepared for immunofluorescence as described above.

Quantification of albumin and urea production

Albumin and urea in spheroid and monolayer supernatant were quantified using Albumin Human ELISA Kit and Urea Assay kit respectively, according to the manufacturer's protocol. Samples were

collected 4 days after media change, twice weekly over 32 days. Data was normalised to account for differences in cell number.

Visualisation of compound penetration

2500 cell spheroids were treated with 3 µg/ml doxorubicin for 24 hours. Spheroids were washed in PBS, fixed in 4 % PFA for 1 hour then incubated with Hoechst diluted 1:5000 in 0.1 % Triton X-100 /1 % BSA in TBST for 1 hour. Spheroids were imaged in 3D by LightSheet fluorescence microscopy (Zeiss LightSheet Z.1).

Hepatotoxin treatment of spheroids

Spheroids were treated at day 3 of culture with hepatotoxic compounds acetaminophen, fialuridine, diclofenac and trovafloxacin diluted in 0.5 % DMSO in EMEM for 4 days with repeat dosing on day 2. Monolayer C3A cells were treated with compounds for 24 hours, as these cells are not healthy if cultured in a confluent monolayer for 4 days. Cell viability was analysed using Cell Titer-Glo assay (Promega) according to the manufacturer's instructions and plotted as a percentage of untreated control.

Statistical analysis

All data were obtained from a minimum of 3 separate repeats in triplicate and represented as mean ± standard error.

Results

Optimisation of Spheroid Starting Cell Number

We assessed how different starting cell numbers may affect spheroid formation, size and shape over time. Spheroids were formed on liquid-overlay plates from a starting cell number of 500, 750, 1000, 1500, 2000 and 2500 C3A cells and cultured for 32 days. Brightfield microscopy was used to measure spheroid diameter and shape twice weekly (Figure 1).

All starting cell numbers resulted in the formation of spheroids of varying sizes, with all of the cells in each well aggregating to form a single spheroid. Spheroids created from 500 cells gradually increased in diameter over 32 days from 237.0 ± 14.3 nm to 432.9 ± 111.4 nm in diameter, however these spheroids were less uniform and less stable in shape, resulting in disaggregation of some cells (Figure 1A and 1B). However, spheroids with a starting cell number of 750 or 1000 cells steadily grew over 32 days, 289.4 ± 26.5 nm and 343.2 ± 73.3 nm at day 4 and increasing to 407.7 ± 92.3 nm and 539.5 ± 39.5 nm at day 32 respectively, and maintained a uniform spherical shape over the course of the culture. Spheroids created with higher starting cell numbers, 1500, 2000 or 2500 cells, increased in diameter more rapidly, reaching much larger diameters of 624.5 ± 59.5 nm, 730.0 ± 112.0 nm and 759.1 ± 83.5 nm, as well as becoming irregular in shape (Figure 1A and 1B). From this data, 750 cells was determined to be an optimal cell number for creating spheroids, as these spheroids stayed the

most uniform in shape over 32 days, with little variation in size and the smallest diameter. 2500 cell spheroids have been subsequently used in our analysis as a comparison.

Internal Spheroid Structure

In order to analyse the internal structure, H&E staining was performed on spheroids with 750 and 2500 cell starting numbers to visualise internal cell morphology and arrangement over 32 days (Figure 2). Staining of spheroids with a starting cell number 750 cells revealed a compact, uniform structure within the spheroids, with a defined outer perimeter (Figure 2). Cells within the spheroids had a cuboidal 3D morphology with direct cell-cell contacts, as seen in the liver *in vivo*. Correlating with cell growth data, the 750 cell spheroids are seen to gradually increase in size, and stay uniformly spherical with limited degrees of necrosis up to day 32. However in the larger 2500 cell spheroids small patches of cell death started to occur around day 14 and, by day 18, a necrotic core had formed. Additionally, by day 25 the 2500 cell spheroids became misshapen and their growth started to rapidly increase, resulting in the spheroids disaggregating and losing structural integrity (Figure 2).

Proliferation of the cells inside the spheroid was analysed over the first 18 days of culture using Ki-67 staining in spheroids with 750 and 2500 starting cell numbers (Figure 3A). Nuclei stain blue with haematoxylin and proliferating cells appear brown, stained with Ki-67. At day 4, 59.50 ± 3.5 % and 50.60 ± 2.3 % of the cells in the spheroids were proliferating for 750 and 2500 starting cell numbers respectively (Figure 3A and 3B). After 18 days in culture, fewer cells were seen to be proliferating, 32.43 ± 6.1 % and 7.40 ± 1.3 % respectively, with proliferating cells mainly located nearer to the periphery of the spheroid (Figure 3A).

The liver lobule can be classed as three regions, periportal, transitional and perivenous regions which display zonation due to the gradient of oxygen and nutrients available from the sinusoidal microvessels (Bacon. BR et al. 2006). CPS1 can be utilised as a zonation marker for periportal areas of the liver (Koenig et al. 2007). We stained spheroids cultured for 18 days for CPS1 and found that it was expressed near the periphery of the spheroid, an area with the highest oxygen concentrations, similar to the periportal area of the liver lobule (Figure 4).

Cellular Polarisation in Spheroids.

One of the key features of hepatocytes is their ability to polarise. This involves the formation of bile canaliculi between adjacent cells, as well as the correct localisation of key transporters to either the apical or canalicular membranes (Gissen and Arias 2015; Godoy et al. 2013). We used immunofluorescence to analyse the internal structure of the spheroids over time. Spheroids were fixed and stained with phalloidin (red) to visualise F-actin structures, by confocal microscopy (Figure 5). After 4 days of culture, F-actin filaments were observed forming between cells within the spheroid (Figure 5A). After 11 days in culture, these larger structures could be seen joining together to create a network throughout the spheroid (Figure 5B).

MRP2 and Pgp are transporters localised to the canalicular membrane of hepatocytes and transport organic anions and efflux lipophilic cations from the cell respectively (Esteller 2008). The expression of these transporters were therefore used to confirm whether the actin structures observed were the result of cellular polarisation and the formation of bile canaliculi, and whether or not culture time affected this process. Spheroids and 2D cultured C3A cells were analysed over 18 days for MRP2 (Figure 6A) and Pgp (Figure 6B) expression. The staining pattern of these transporters emulated that seen with the phalloidin (Figure 5). The secondary structures could be seen forming after 4 days of culture regardless of the starting cell number (supplementary information), and appeared to elongate and join together over time, forming an interconnected network of canalicular structures (Figure 6). The same staining pattern for MRP2 and Pgp was not seen in a 2D monolayer culture (Figure 6).

Confirmation of Liver-Like Function in Spheroids

Transporter functionality was determined using fluorescently labelled CMFDA. This compound can passively enter cells but can only be effluxed from cells via active transport through MRP2. 2D monolayer C3A cells retained CMFDA (green) within the cell cytoplasm (Figure 7). However in the spheroids there was limited retention of CMFDA within cell cytoplasm and an accumulation and co-localisation of the compound within secondary canalicular-like structures, shown by F-actin in red (Figure 7). This suggests that in the spheroids CMFDA was actively transported out of the cells and into the secondary structures, indicating functional MRP2 transporters on the canalicular membrane.

In order to determine the presence of key liver-specific enzymes we stained for CYP2E1, an important metabolic enzyme in the liver. CYP2E1 was clearly observed throughout the spheroid, indicating that the spheroids express this liver-specific functional marker (Figure 8).

Albumin and urea production from spheroids was quantified over 32 days. Albumin production gradually increased from 36.96 ± 15.5 ng/ml at day 4 of culture to 878.92 ± 349.6 ng/ml at day 32 (Figure 13A). We compared this to 2D monolayer cultured C3A cells which were seen to produce a maximum 82.31 ± 5.38 ng/ml albumin. Similarly, urea production steadily increased over 32 days from 6.20 ± 1.9 nmol/ml to 21.71 ± 2.0 nmol/ml (Figure 13B). In monolayer cultured C3A cells a maximum of 2.62 ± 0.15 nmol/ml urea was produced.

Drug penetration throughout the spheroid

The assessment of acute and chronic drug toxicity is one of the key applications of 3D spheroids. We next wanted to confirm compound penetration and ascertain whether or not all the cells within the spheroids are being exposed to compounds added exogenously. 11 day old 750 cell spheroids, estimated to be around 263 μm from the data in Figure 1B, were treated with doxorubicin, an autofluorescent chemotherapeutic compound with a molecular mass of 543 g/mol and a LogP of 1.27, and imaged using LightSheet microscopy in order to analyse compound penetration throughout the entire spheroids. Separate images were taken throughout the z-plane of the spheroid to visualise throughout the entire spheroid core. Figure 10 shows the spheroid after treatment with doxorubicin (green) for 24 hours, with nuclei shown in blue. Doxorubicin can be seen fluorescing throughout the

spheroid core in the median section through the spheroid (Figure 10A), as well as throughout the periphery (Figure 10B), thus confirming that this compound is in contact with every cell in the spheroid and that the drug response observed is present within all cells.

Toxicological analysis

Spheroids and 2D monolayer C3A cells were treated with varying concentrations of hepatotoxic compounds and cell viability analysed. A 4 day repeat dosing strategy could be used for spheroid cultures, however only 24 hour treatment of monolayers was performed in order to avoid cells becoming over confluent and necrotic. Dose-dependent toxicity was observed in the spheroids in response to all hepatotoxins (Figure 11). Paracetamol had an IC_{50} value of 8605 µM in spheroids (Figure 11A), significantly lower than that found in a standard 2D monolayer culture, reported to be 22800 µM (Ju et al. 2015). Similarly diclofenac has a reported IC_{50} value of 763 µM (Lin and Will 2012) in HepG2 monolayer cultures, whereas it was significantly lower in our spheroid model, at 305 µM (Figure 11B). The final two hepatotoxic compounds, troglitazone and nefazodone, also had a lower IC_{50} in spheroids at 34.2 µM and 15 µM respectively (Figure 11C and 11D) compared to 121.2 µM and 20.2 µM reported in monolayer cultures (Lin and Will 2012).

Statistical analysis

All data were obtained from a minimum of 3 separate repeats in duplicate or more and represented as mean ± standard error.

Discussion

3D *in vitro* models are becoming more widely used when investigating drug toxicity. Multiple companies now offer spheroids to be shipped ready for use in drug toxicity testing. Research has shown the potential for liver spheroid models to predict hepatotoxicity more precisely than commonly used 2D liver models, as well as spheroids being more amenable to high-throughput screening and long-term repeat dose studies. However the spatiotemporal characteristics and function of liver spheroids over time has not been fully investigated, as well as minimal comparison between the functionality and predictivity of liver spheroids and other 2D models.

We have developed a technique for creating liver spheroids from the C3A cell line. C3A cells, a derivative of HepG2 cells, were chosen for this model as they exhibit strong contact-inhibited growth characteristics, therefore when cultured in a spheroid these cells do not proliferate to the same extent as other hepatocarcinoma cell lines (Wrzesinski and Fey 2013). This emulates primary cells which bear limited proliferation capacity. As with other liver cell lines, C3A cells have disadvantages including limited expression of metabolizing enzymes and lack of liver-specific functions (Guo et al. 2011; LeCluyse et al. 2012), however the advantages over primary cells include unlimited lifespan, stable phenotype and absence of donor variation (Donato et al. 2008; LeCluyse et al. 2012). Other studies have used C3A cells to create spheroids, such as Wrzesinski's group, who created C3A

spheroids on AggreWell plates and cultured them in micro-gravity bioreactor (Fey and Wrzesinski 2012; Wrzesinski and Fey 2013; Wrzesinski et al. 2013). They performed extensive characterisation of their spheroid growth and viability and revealed increases in urea and cholesterol synthesis over 42 days of culture, as well as changes in gene expression (Wrzesinski and Fey 2013; Wrzesinski et al. 2013). We adopted a different scaffold free approach for creating spheroids in order create direct cell-cell contacts and to reduce any ECM effects, which have been shown to dedifferentiate cells, altering their morphology and function (Gomez-Lechon et al. 1998; Semler et al. 2000; Wells 2008).

In this study, we created and characterised uniform, reproducible C3A spheroids using the liquid-overlay technique, which has not been previously reported to have been used to create C3A spheroids. We initially compared the liquid-overlay technique to ultra-low adherence (ULA) plates, another commonly used scaffold-free method of creating spheroids. Despite having similar growth characteristics, spheroids created on ULA plates had a more irregular and non-spherical structure with a less defined outer perimeter compared to those formed using the liquid overlay technique, which were uniform and spherical (Supplementary Figure 1). The liquid-overlay technique was reliable and reproducible, forming uniform spheroids in every experiment in every well, it also does not require an extensive tissue engineering background, making this model more user-friendly than some other systems. The cost-effectiveness of the model and amenability to both high-throughput and repeat-dose studies makes it a promising model for toxicological studies. Spheroids cultured from 750 cells did not develop a necrotic core after 32 days of culture and remained relatively small, with a maximum diameter of 407.8 ± 92.3 nm, and uniformity in shape and size. Proliferation of cells within the spheroids decreased over time, similar to that seen in studies with HepG2 cells (Ramaiahgari et al. 2014). Histological analysis revealed a cuboidal cell morphology within the spheroids, with direct cell-cell contacts similar to an *in vivo* liver structure, unlike in 2D liver cell models where the cells have altered cell morphology, including an elongated and flattened structure, with cell contacts only in one plane, therefore limiting cell signalling (Semler et al. 2000; Wells 2008).

One disadvantage of using spheroids for drug testing is that necrosis can occur within the spheroid core, distorting toxicity data. It has been suggested that oxygen and nutrients can diffuse through tissue approximately 100 µm (Asthana and Kisaalita 2012; Curcio et al. 2007; Olive et al. 1992), however little research has gone in to specifically determining the size or time at which liver spheroids develop necrosis in the core, which may well depend of the cell type, number, scaffold interactions and culture conditions. We have found that using 750 cells is an optimum starting cell number and a culture period of 32 days in which liver spheroids do not possess a necrotic core, reaching a size of approximately 400 µm. Additionally our spheroids recapitulate the zonation of the liver that occurs *in vivo* due to oxygen and nutrient gradients. We confirmed this by staining for the periportal marker CPS1, which is expressed in areas nearest to the oxygenated blood supply in the liver and can be seen staining the peripheral regions on the spheroid in a similar expression pattern, indicating spatiotemporal similarity compared to the human liver (Koenig et al. 2007). A spheroid cultured for 18 days was used for this experiment, as it was estimated from cell growth data to be around 354 µm, sufficiently large for an oxygen gradient to have developed. However we also revealed that once the

C3A spheroids exceed 700 µm in diameter a necrotic core develops, regardless of the culture time (Figure 2). Henceforth, C3A spheroids exceeding this critical size cannot be used to accurately determine the effect of a toxicological compound since they are likely to have a necrotic core which would give unrepresentative results. The size of the spheroid is therefore an essential parameter that should be taken into account in toxicological studies.

In vivo, hepatocytes are structurally and functionally polarised (Gissen and Arias 2015; Godoy et al. 2013), and we have recapitulated this phenotype in our spheroids. Secondary actin structures can be observed forming enhanced networks throughout the spheroids, which has been observed in other studies (Ramaiahgari et al. 2014; Wrzesinski et al. 2014), and we confirmed that these structures were a result of cellular polarisation by staining for MRP2 and Pgp, transporters known to be expressed and localised to the canalicular membrane of hepatocytes *in vivo* (Gissen and Arias 2015). These bile canalicular structures form after 4 days in culture and are present for at least 4 weeks, regardless of spheroid size (Supplementary Figure 2). MRP2 transporter function has been proven in HepG2 spheroids, but has not previously been investigated in a C3A spheroid model. Furthermore, we confirmed that the MRP2 transporters were functional by utilising CMFDA, which is membrane permeable, however once inside cells it is converted to glutathione-methylfluorescein (GSMF), a membrane impermeable compound which can only be excreted from cells via transport through function MRP2 transporters. We witnessed accumulation of CMFDA in bile canalicular structures in spheroids, with little remaining within the cell, indicating that MRP2 transporters in the spheroid are functional. As another liver-specific marker we stained for CYP2E1 (Koenig et al. 2007), an important metabolic enzyme, which was confirmed to be expressed throughout the spheroid at day 18. In HepG2 spheroids CYP2E1 has been shown to have maximal expression on day 21 to 28 of culture (Ramaiahgari et al. 2014). We additionally confirmed that the spheroids were able to synthesise and secrete albumin and urea, with a gradual increase in production over 32 days of culture, with around ten times more albumin and urea produced in spheroids than 2D monolayer cultured C3A cells. This again indicates liver specific functionality in the spheroids, as albumin and urea production are important physiological functions of hepatocytes *in vivo,* and builds on the evidence that cells cultured in spheroids have superior functionality to those cultured in 2D. (Lippincott. J. B 1993).

One complication when comparing 2D monocultures to spheroids is whether or not the cells in both models are exposed to the same concentrations of drug compounds. By using LightSheet microscopy we have confirmed that the chemotherapeutic drug doxorubicin can penetrate into cells in the core of a spheroid with a diameter of around 263 µm. This allows us to assume that all cells within the treated spheroids were exposed to similar concentrations of doxorubicin, although the exact concentration cannot be quantified using this technique. We can however predict that other compounds with similar physicochemical properties to doxorubicin (molecular mass 543 g/mol, LogP of 1.27) would also be able to penetrate the C3A spheroids, enabling us to utilise this model for drug toxicology studies. We analysed the toxicological predictivity of our C3A spheroids compared to reported data obtained from standard 2D monolayer cultures of HepG2 cells. At day 3 of culture spheroids were treated with compounds for 4 days utilising a repeat dosing strategy, and we have previously shown that

spheroids are viable with no pre-existing necrosis during this culture time. We calculated the IC_{50} values, as this is an industry standard for determining whether or not an *in vitro* model can detect hepatotoxicity. Spheroids were found to be more susceptible to toxicity from these hepatotoxic compounds than 2D cultures, indicated by lower IC_{50} values in the spheroid model. This suggests that the 3D spheroid model is more sensitive to hepatotoxins and better at predicting whether or not a compound is likely to cause hepatotoxicity.

Conclusion

Spheroids have promise to be adopted as an *in vitro* liver model for safety screening, including enhanced functional lifespan for repeat-dose studies, structural similarities with *in vivo*, good reproducibility and amenability to high-throughput screening. We have successfully developed a reproducible technique for creating uniform C3A spheroids and characterised their growth and proliferation characteristics over 32 days. Our spheroids have an *in vivo*-like structure including limited necrosis, zonation and polarised cells, as well as liver-specific functions such as the ability to synthesise and secrete albumin and urea, functional canalicular transporters and CYP2E1 expression. An initial drug screen indicated that our spheroid model can predict the toxicity of hepatotoxic compounds with a higher sensitivity than standard 2D monolayer cultures.

Acknowledgements

The authors would like to thank the Medical Research Council and AstraZeneca for funding this project. We acknowledge the Liverpool Centre for Cell Imaging (CCI) for provision of imaging equipment and technical assistance. We would also like to thank Marco Marcello for help with technical assistance and image analysis support. We would like to thank the Julie Haigh at the Department of Veterinary Pathology, Leahurst Campus, University of Liverpool for immunohistochemistry of spheroids.

Asthana A, Kisaalita WS (2012) Microtissue size and hypoxia in HTS with 3D cultures. Drug discovery today 17(15-16):810-7 doi:10.1016/j.drudis.2012.03.004

Bacon. BR, O'grady. JG, Di bisceglie. AM, JR. L (2006) Comprehensive clinical hepatology. Elsevier Health Sciences

Chang TT, Hughes-Fulford M (2009) Monolayer and spheroid culture of human liver hepatocellular carcinoma cell line cells demonstrate distinct global gene expression patterns and functional phenotypes. Tissue engineering Part A 15(3):559-67 doi:10.1089/ten.tea.2007.0434

Colley HE, Hearnden V, Jones AV, et al. (2011) Development of tissue-engineered models of oral dysplasia and early invasive oral squamous cell carcinoma. British journal of cancer 105(10):1582-92 doi:10.1038/bjc.2011.403

Curcio E, Salerno S, Barbieri G, De Bartolo L, Drioli E, Bader A (2007) Mass transfer and metabolic reactions in hepatocyte spheroids cultured in rotating wall gas-permeable membrane system. Biomaterials 28(36):5487-97 doi:10.1016/j.biomaterials.2007.08.033

Donato MT, Lahoz A, Castell JV, Gomez-Lechon MJ (2008) Cell lines: a tool for in vitro drug metabolism studies. Current drug metabolism 9(1):1-11
Esteller A (2008) Physiology of bile secretion. World J Gastroentero 14(37):5641-5649 doi:Doi 10.3748/Wjg.14.5641
Fey SJ, Wrzesinski K (2012) Determination of drug toxicity using 3D spheroids constructed from an immortal human hepatocyte cell line. Toxicological sciences : an official journal of the Society of Toxicology 127(2):403-11 doi:10.1093/toxsci/kfs122
Friedrich J, Seidel C, Ebner R, Kunz-Schughart LA (2009) Spheroid-based drug screen: considerations and practical approach. Nature protocols 4(3):309-24 doi:10.1038/nprot.2008.226
Gissen P, Arias IM (2015) Structural and functional hepatocyte polarity and liver disease. J Hepatol 63(4):1023-37 doi:10.1016/j.jhep.2015.06.015
Godoy P, Hewitt NJ, Albrecht U, et al. (2013) Recent advances in 2D and 3D in vitro systems using primary hepatocytes, alternative hepatocyte sources and non-parenchymal liver cells and their use in investigating mechanisms of hepatotoxicity, cell signaling and ADME. Archives of toxicology 87(8):1315-530 doi:10.1007/s00204-013-1078-5
Gomez-Lechon MJ, Donato MT, Castell JV, Jover R (2004) Human hepatocytes in primary culture: the choice to investigate drug metabolism in man. Current drug metabolism 5(5):443-62
Gomez-Lechon MJ, Jover R, Donato T, et al. (1998) Long-term expression of differentiated functions in hepatocytes cultured in three-dimensional collagen matrix. Journal of cellular physiology 177(4):553-62 doi:10.1002/(SICI)1097-4652(199812)177:4<553::AID-JCP6>3.0.CO;2-F
Guo L, Dial S, Shi L, et al. (2011) Similarities and differences in the expression of drug-metabolizing enzymes between human hepatic cell lines and primary human hepatocytes. Drug metabolism and disposition: the biological fate of chemicals 39(3):528-38 doi:10.1124/dmd.110.035873
Ju SM, Jang HJ, Kim KB, Kim J (2015) High-Throughput Cytotoxicity Testing System of Acetaminophen Using a Microfluidic Device (MFD) in HepG2 Cells. Journal of toxicology and environmental health Part A 78(16):1063-72 doi:10.1080/15287394.2015.1068650
Khetani SR, Berger DR, Ballinger KR, Davidson MD, Lin C, Ware BR (2015) Microengineered Liver Tissues for Drug Testing. Journal of laboratory automation doi:10.1177/2211068214566939
Koenig S, Aurich H, Schneider C, et al. (2007) Zonal expression of hepatocytic marker enzymes during liver repopulation. Histochemistry and cell biology 128(2):105-14 doi:10.1007/s00418-007-0301-y
Lazarou J, Pomeranz BH, Corey PN (1998) Incidence of adverse drug reactions in hospitalized patients: a meta-analysis of prospective studies. Jama 279(15):1200-5 doi:jma71005 [pii]
LeCluyse EL, Alexandre E, Hamilton GA, et al. (2005) Isolation and culture of primary human hepatocytes. Methods in molecular biology 290:207-29
LeCluyse EL, Witek RP, Andersen ME, Powers MJ (2012) Organotypic liver culture models: meeting current challenges in toxicity testing. Critical reviews in toxicology 42(6):501-48 doi:10.3109/10408444.2012.682115
Lin Z, Will Y (2012) Evaluation of drugs with specific organ toxicities in organ-specific cell lines. Toxicological sciences : an official journal of the Society of Toxicology 126(1):114-27 doi:10.1093/toxsci/kfr339
Lippincott. J. B (1993) Diseases of the Liver, 7 edn. Wiley-Blackwell
Nibourg GA, Chamuleau RA, van Gulik TM, Hoekstra R (2012) Proliferative human cell sources applied as biocomponent in bioartificial livers: a review. Expert opinion on biological therapy 12(7):905-21 doi:10.1517/14712598.2012.685714
Norris W, Paredes AH, Lewis JH (2008) Drug-induced liver injury in 2007. Current opinion in gastroenterology 24(3):287-97 doi:10.1097/MOG.0b013e3282f9764b
Olive PL, Vikse C, Trotter MJ (1992) Measurement of oxygen diffusion distance in tumor cubes using a fluorescent hypoxia probe. International journal of radiation oncology, biology, physics 22(3):397-402

Peshwa MV, Wu FJ, Sharp HL, Cerra FB, Hu WS (1996) Mechanistics of formation and ultrastructural evaluation of hepatocyte spheroids. In vitro cellular & developmental biology Animal 32(4):197-203

Ramaiahgari SC, den Braver MW, Herpers B, et al. (2014) A 3D in vitro model of differentiated HepG2 cell spheroids with improved liver-like properties for repeated dose high-throughput toxicity studies. Archives of toxicology 88(5):1083-95 doi:10.1007/s00204-014-1215-9

Reuben A, Koch DG, Lee WM, Acute Liver Failure Study G (2010) Drug-induced acute liver failure: results of a U.S. multicenter, prospective study. Hepatology 52(6):2065-76 doi:10.1002/hep.23937

Sainz B, Jr., TenCate V, Uprichard SL (2009) Three-dimensional Huh7 cell culture system for the study of Hepatitis C virus infection. Virology journal 6:103 doi:10.1186/1743-422X-6-103

Semler EJ, Ranucci CS, Moghe PV (2000) Mechanochemical manipulation of hepatocyte aggregation can selectively induce or repress liver-specific function. Biotechnology and bioengineering 69(4):359-69

Takahashi Y, Hori Y, Yamamoto T, Urashima T, Ohara Y, Tanaka H (2015) 3D spheroid cultures improve the metabolic gene expression profiles of HepaRG cells. Bioscience reports 35(3) doi:10.1042/BSR20150034

Tostoes RM, Leite SB, Serra M, et al. (2012) Human liver cell spheroids in extended perfusion bioreactor culture for repeated-dose drug testing. Hepatology 55(4):1227-36 doi:10.1002/hep.24760

van Zijl F, Mikulits W (2010) Hepatospheres: Three dimensional cell cultures resemble physiological conditions of the liver. World journal of hepatology 2(1):1-7 doi:10.4254/wjh.v2.i1.1

Wang Z, Luo X, Anene-Nzelu C, et al. (2015) HepaRG culture in tethered spheroids as an in vitro three-dimensional model for drug safety screening. Journal of applied toxicology : JAT 35(8):909-17 doi:10.1002/jat.3090

Wells RG (2008) The role of matrix stiffness in regulating cell behavior. Hepatology 47(4):1394-400 doi:10.1002/hep.22193

Wong SF, No da Y, Choi YY, Kim DS, Chung BG, Lee SH (2011) Concave microwell based size-controllable hepatosphere as a three-dimensional liver tissue model. Biomaterials 32(32):8087-96 doi:10.1016/j.biomaterials.2011.07.028

Wrzesinski K, Fey SJ (2013) After trypsinisation, 3D spheroids of C3A hepatocytes need 18 days to re-establish similar levels of key physiological functions to those seen in the liver. Toxicology Research 2(2):123-135 doi:10.1039/c2tx20060k

Wrzesinski K, Magnone MC, Hansen LV, et al. (2013) HepG2/C3A 3D spheroids exhibit stable physiological functionality for at least 24 days after recovering from trypsinisation. Toxicology Research 2(3):163-172 doi:10.1039/c3tx20086h

Wrzesinski K, Rogowska-Wrzesinska A, Kanlaya R, et al. (2014) The cultural divide: exponential growth in classical 2D and metabolic equilibrium in 3D environments. PloS one 9(9):e106973 doi:10.1371/journal.pone.0106973

Yuhas JM, Li AP, Martinez AO, Ladman AJ (1977) A Simplified Method for Production and Growth of Multicellular Tumor Spheroids. Cancer Research 37:3639-3643

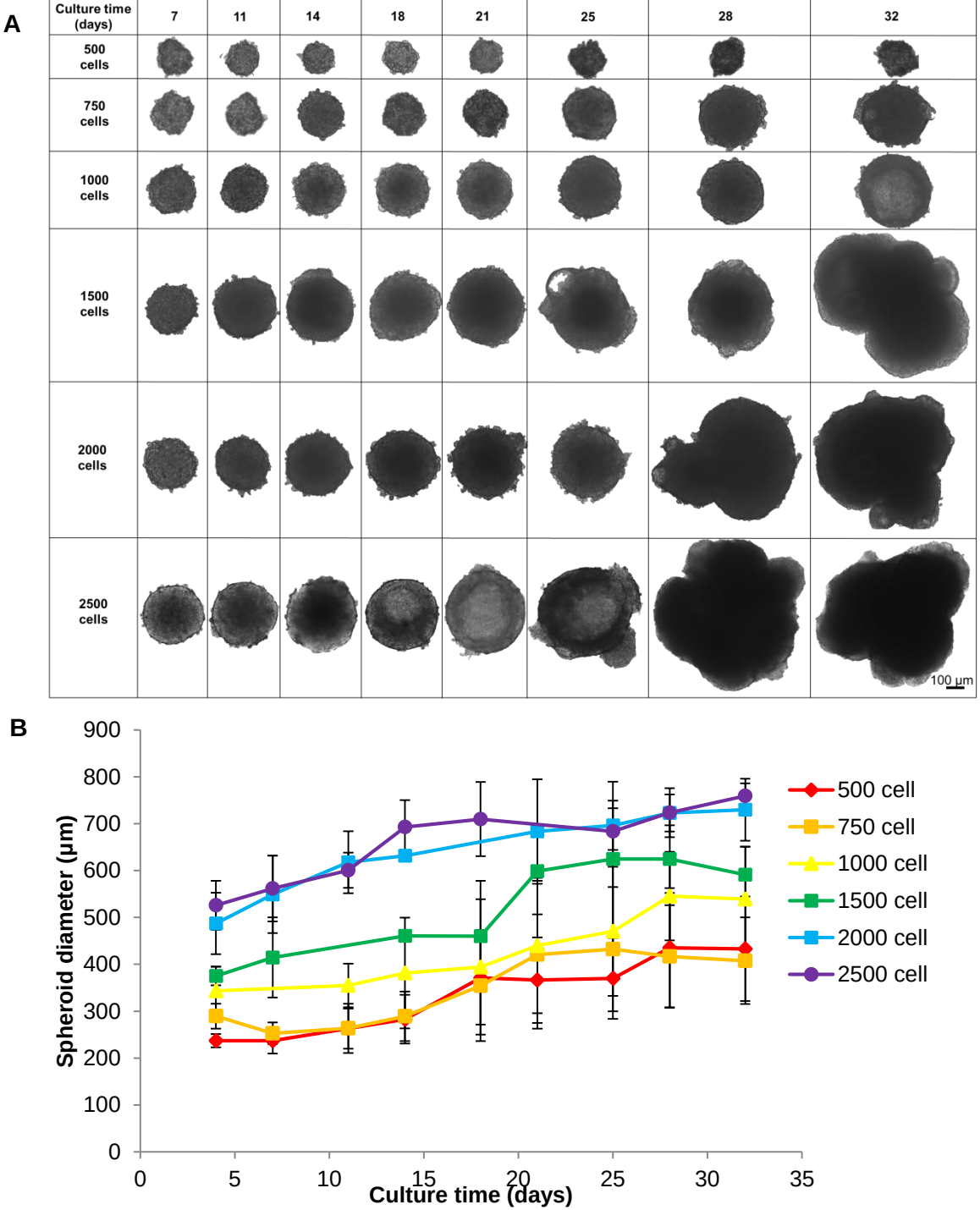

Figure 1. Effect of starting cell number on spheroid formation, size and shape. *Spheroids were created from starting cell numbers 500, 750, 1000, 1500, 2000 and 2500 C3A cells and cultured for 32 days. (**A**) Phase-contrast images of spheroids, images taken at day 7, 11, 14, 18, 21, 25, 28, 32. Scale bar = 100 µm. (**B**) Growth curve of spheroids, diameter measured over 32 days. Spheroid diameter (µm) was plotted against culture time (days). Data are represented as mean ± standard error (n=3 in triplicate).*

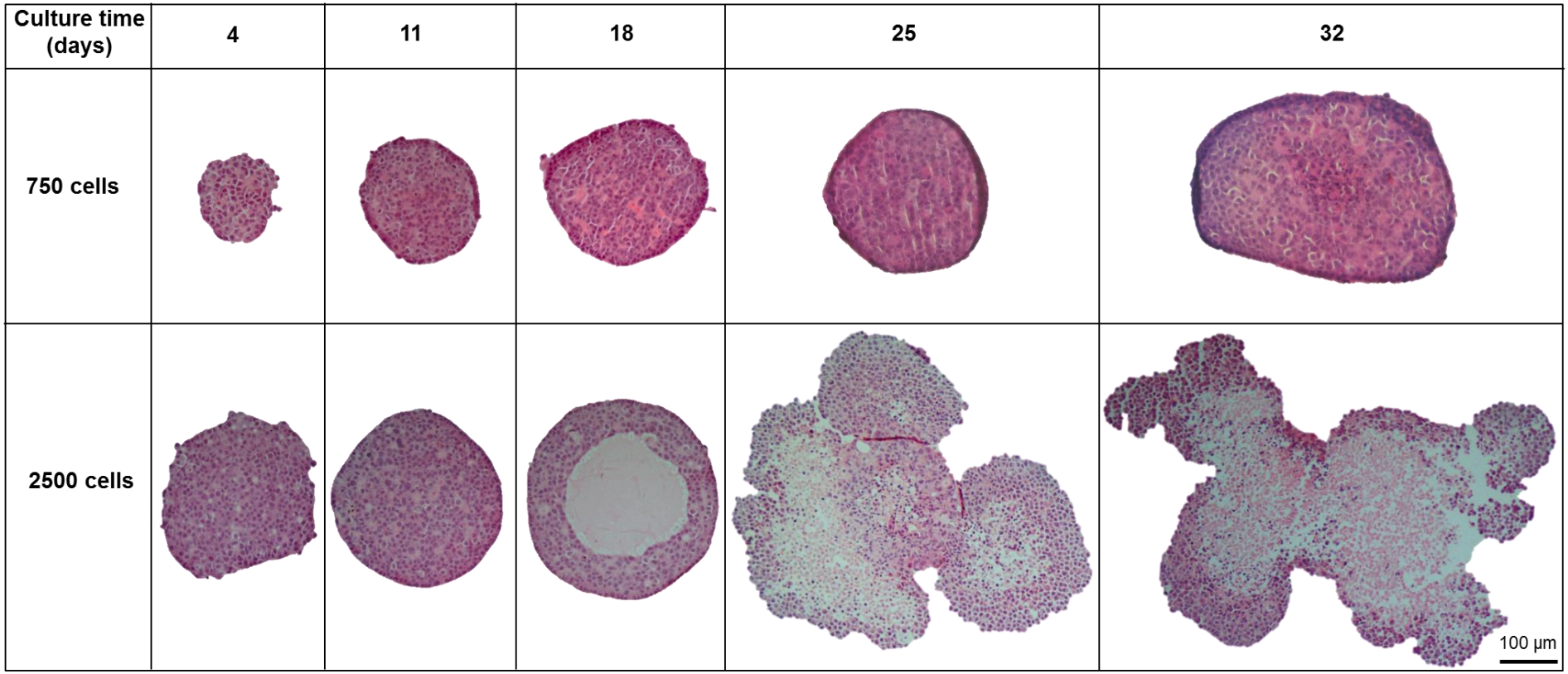

Figure 2. Internal structure of spheroids over time. *Spheroids were created on liquid-overlay plates from 750 or 2500 C3A cells and fixed at day 4, 11, 18, 25 and 32 of culture, paraffin embedded then sectioned and stained with haematoxylin and eosin. Images taken on X microscope. Scale bar = 100 µm.*

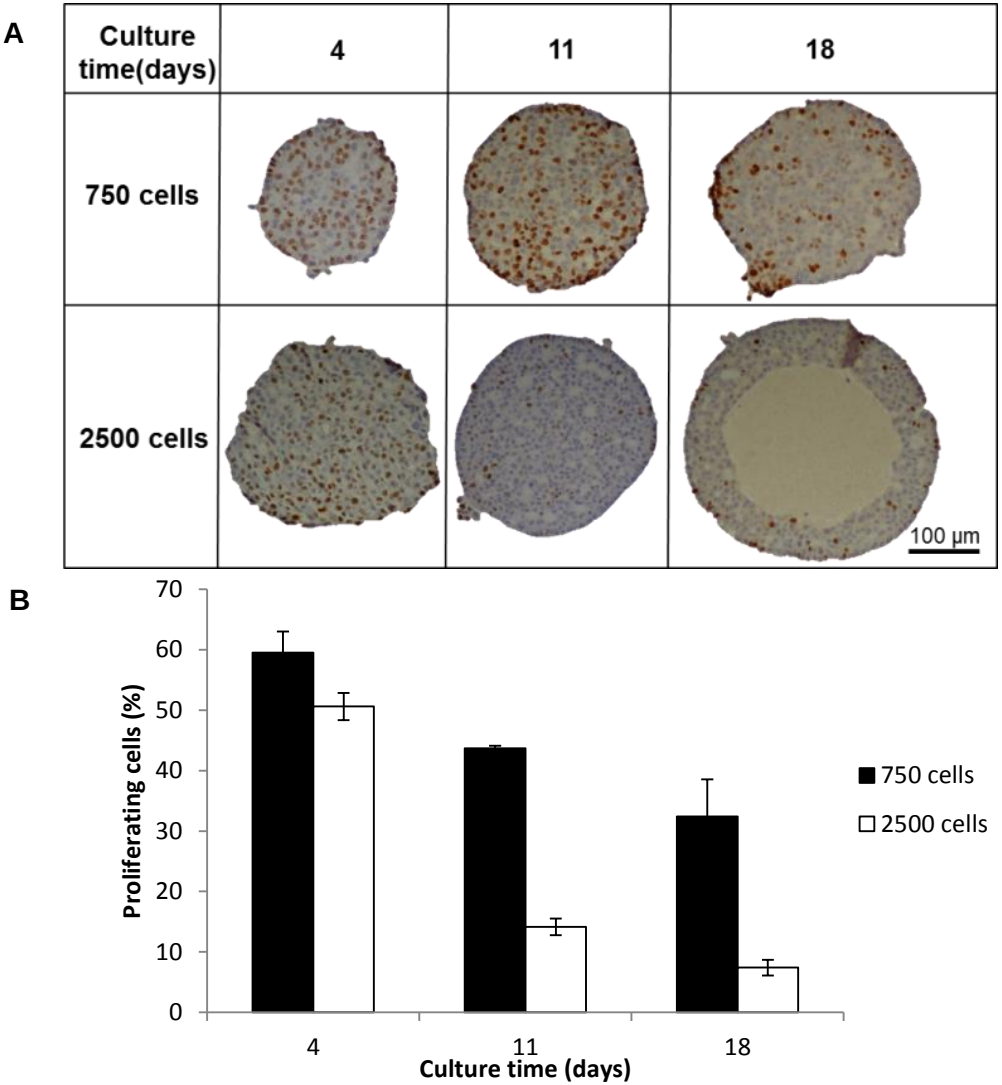

Figure 3. Proliferation of spheroids over time. *Spheroids were created on liquid-overlay plates from 750 or 2500 C3A cells and fixed at day 4, 11 and 18 of culture, paraffin embedded then sectioned and stained with ki67 and haematoxylin. (**A**) Images of spheroid sections stained with Ki-67 and haematoxylin, taken on X microscope. Scale bar =100 µm; (**B**) Bar chart showing proliferating cells (%) plotted against time of culture (days). Data are represented as mean ± standard error (n=3).*

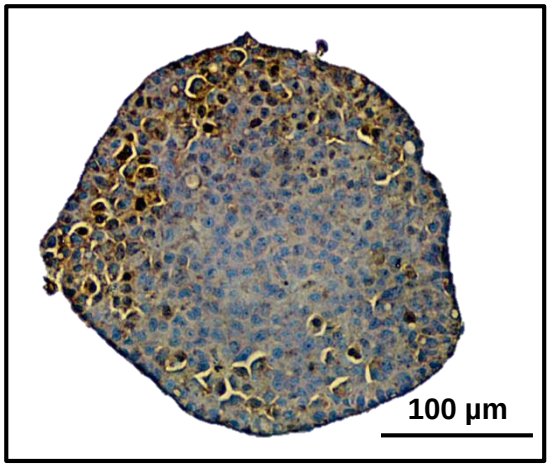

Figure 4. Zonation of spheroids. *Spheroids were created on liquid-overlay plates from 750 cells and fixed at day 18 of culture, paraffin embedded then sectioned and stained with CPS1 a periportal marker. Scale bar =100 µm.*

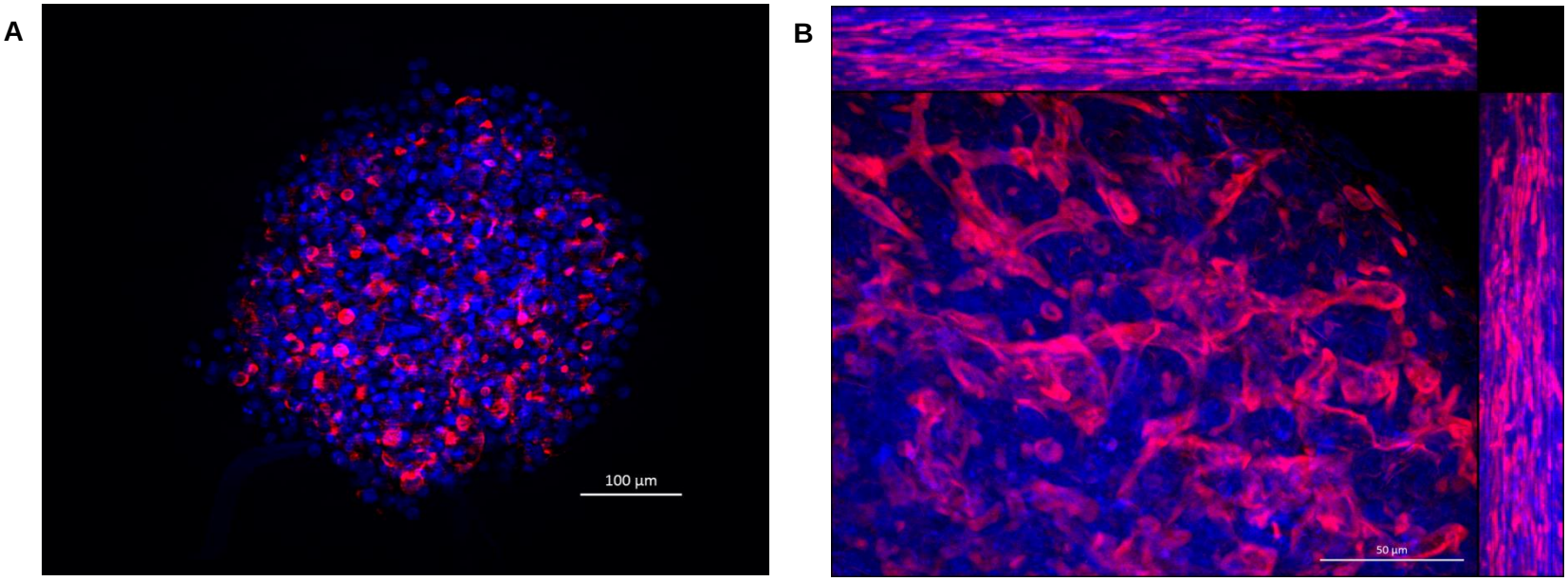

Figure 5. Secondary structures form in spheroids. *Spheroids were cultured on liquid-overlay plates for (**A**) 4 days or; (**B**) 18 days, fixed and stained with Hoechst (blue) to stain the nuclei and phalloidin (red) to stain F-actin, and imaged by confocal microscopy and represented as maximum intensity projection images. Scale bars = 100 µm and 50 µm respectively.*

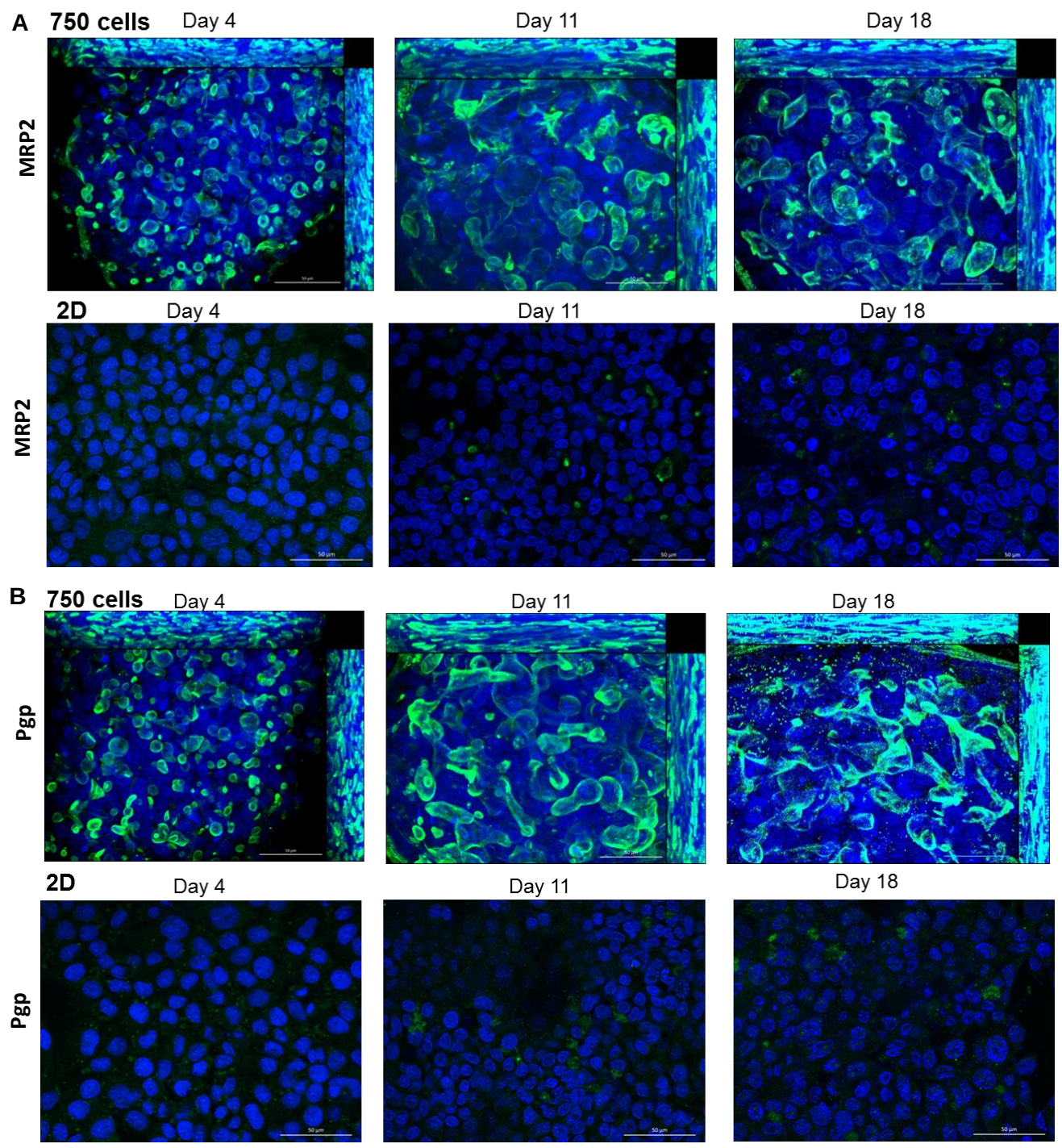

Figure 6. Cell polarisation and transporter localisation in spheroids. *Spheroids were created from 750 C3A cells by liquid-overlay technique or C3A cells were cultured in a 2D monolayer and fixed at day 4, 11 and 18 of culture. Immunofluorescent staining was performed for the canalicular transporter (**A**) MRP2 (green) or; (**B**) Pgp (green) and Hoechst (blue) to stain the nuclei, and imaged by confocal microscopy and represented as maximum intensity projection images. Scale bars = 50 µm.*

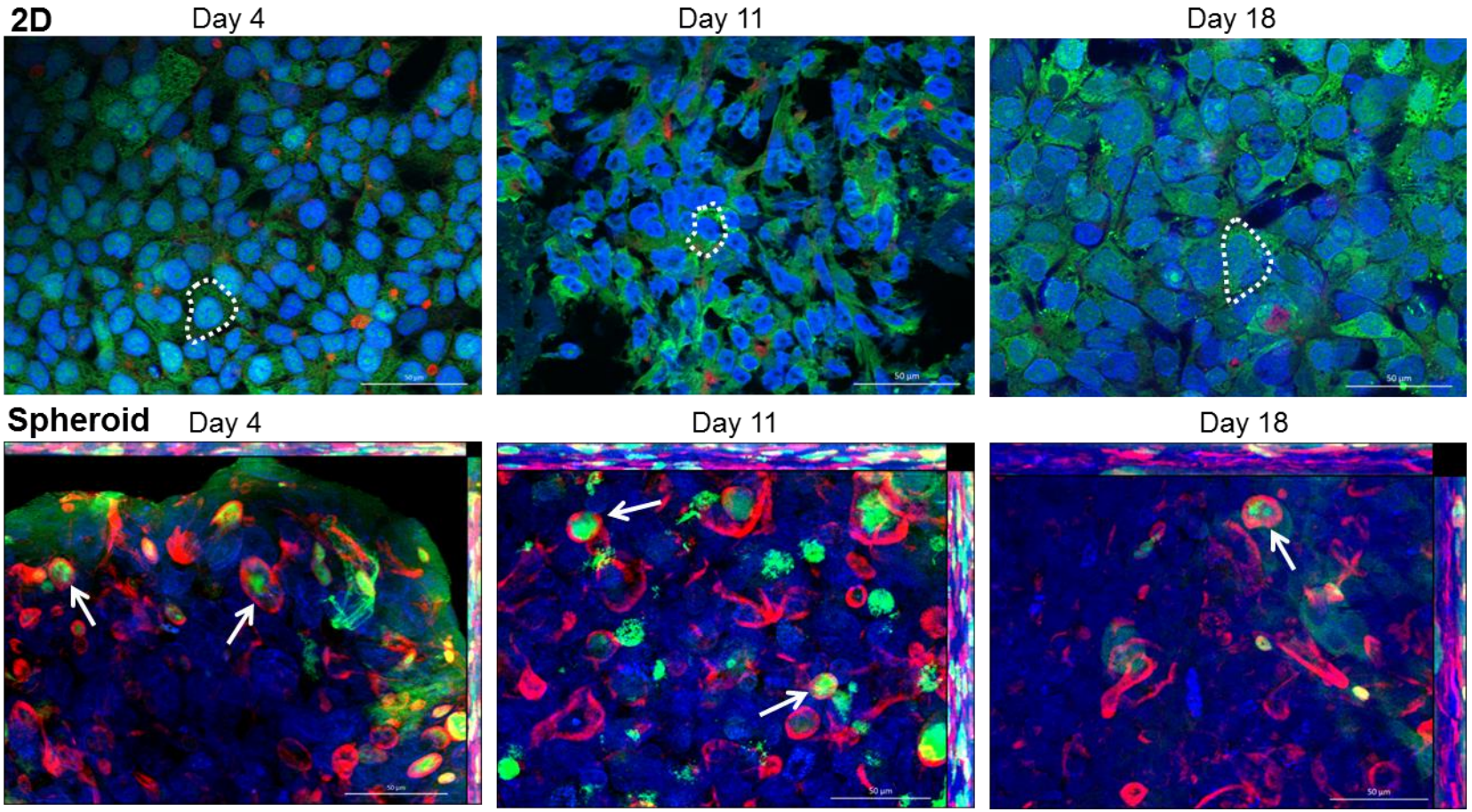

Figure 7. Accumulation of CMFDA in canalicular structures in spheroids. *Spheroids were created from 750 C3A cells on liquid-overlay plates or C3A cells were cultured in a 2D monolayer on glass coverslips for 4, 11 or 18 days and then incubated with CMFDA (green) for 30 min, washed, fixed and stained with Hoechst (blue) to stain the nuclei and phalloidin (red) to stain F-actin, and imaged by confocal microscopy, represented as maximum intensity projection images. Dotted line indicates an example of a cell where CMDFA is retained within the cell cytoplasm. Arrow indicates the canalicular-like structures containing CMFDA. Scale bars = 50 µm.*

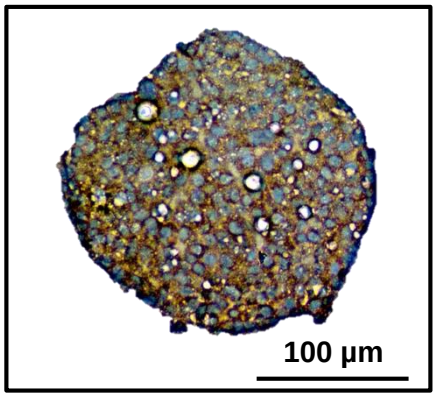

Figure 8. CYP enzyme expression in spheroids. *Spheroids were created on liquid-overlay plates from 750 cells and fixed at day 11 of culture, paraffin embedded then sectioned and stained with CYP2E1. Scale bar =100 µm.*

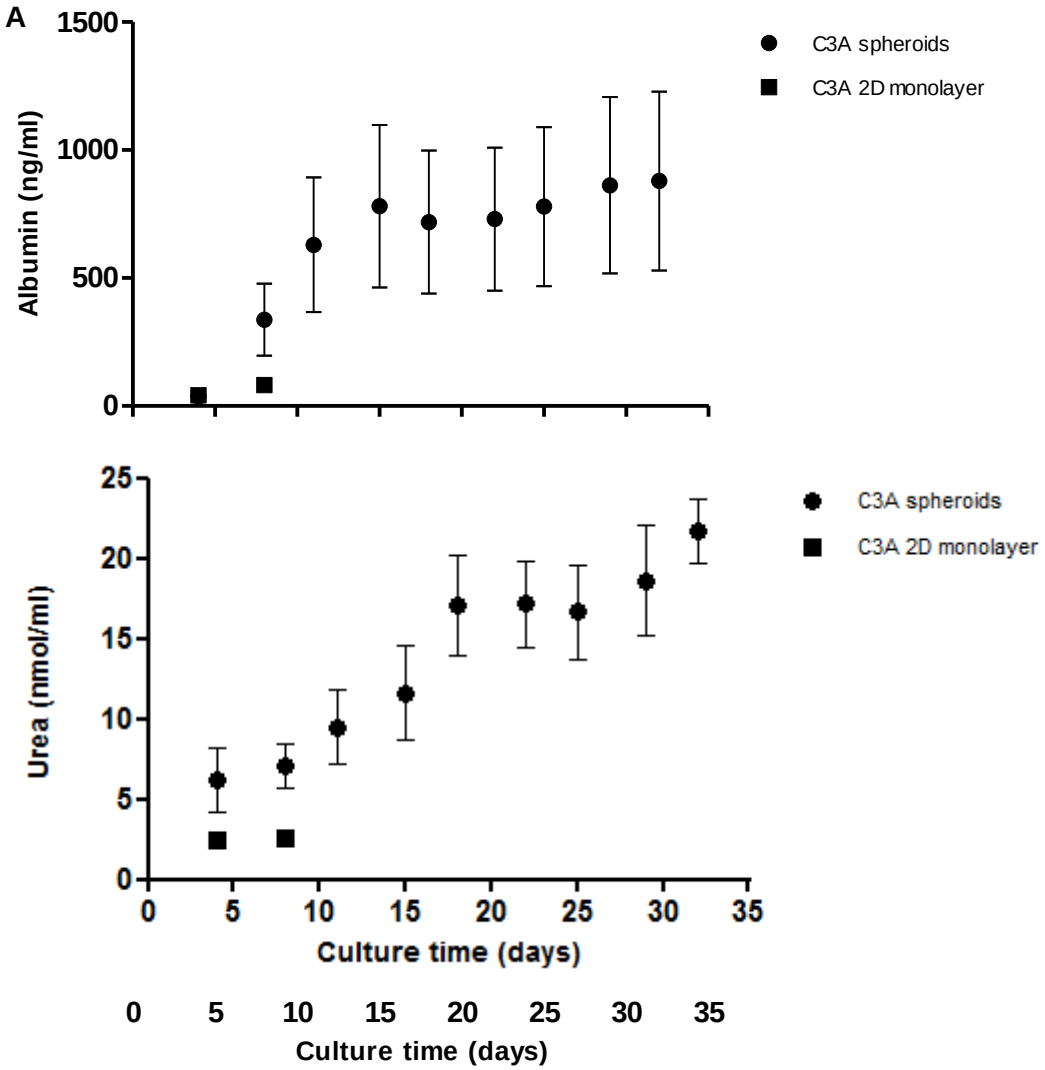

Figure 9. Albumin and urea production in spheroids. *Spheroids were created from 1000 C3A cells on liquid-overlay plates and C3A monolayer cultures used as a comparison. Supernatant samples were taken twice weekly over 32 days and albumin and urea release were quantified. (**A**) Albumin and, (**B**) urea release were quantified and plotted again culture time (days). Data are represented as mean ± standard error (n=3).*

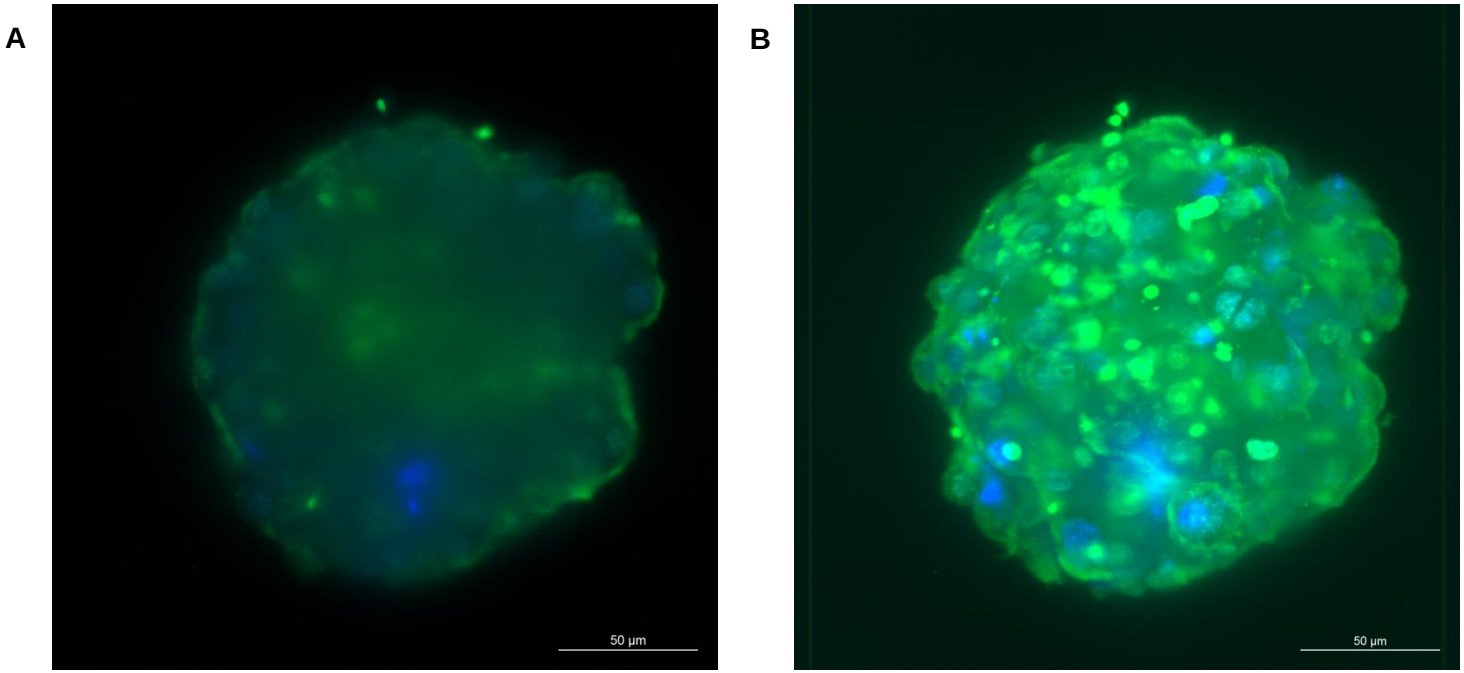

Figure 10. Drug penetration throughout the spheroid. *Spheroids were cultured on liquid-overlay plates for 11 days, treated with 3 µg/ml doxorubicin (green) for 24 hours, fixed, stained with Hoechst (blue) to stain the nuclei and imaged by LightSheet microscopy. (**A**) Represents a median section through the spheroid and; (**B**) a maximum projection image. Scale bars = 50µm.*

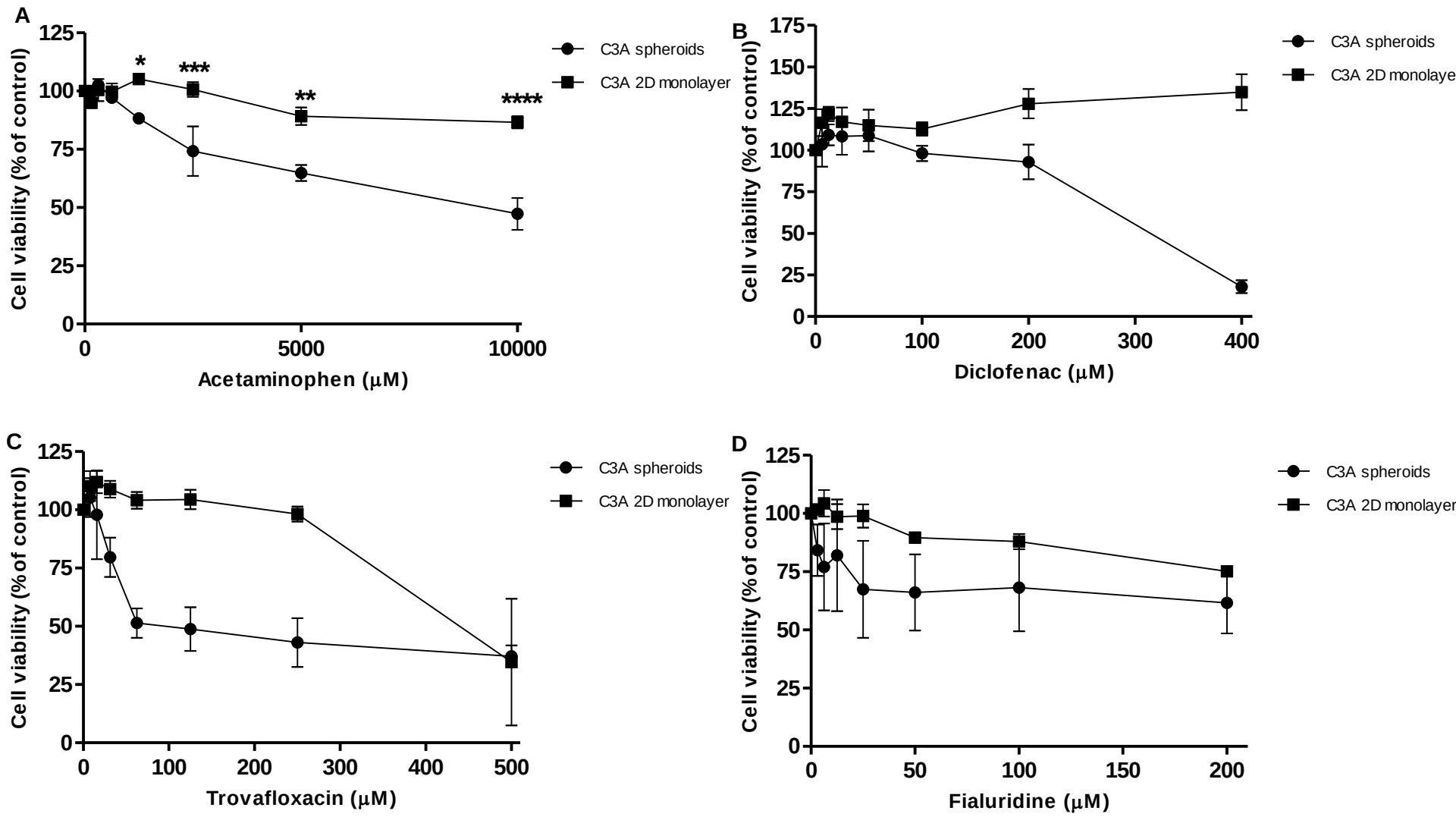

Figure 2.16. Spheroids show a toxic response to hepatotoxins. *Spheroids were created from 1000 C3A cells by liquid-overlay technique, using 2D monolayer C3A cells as a comparison, and treated with (**A**) acetaminophen; (**B**) diclofenac; (**C**) trovafloxacin and (**D**) fialuridine. Cell viability was analysed and plotted as a percentage of untreated control. Data are represented as mean ± standard error (n=3).*

Compound	IC_{50} value in C3A spheroids (μM)	IC_{50} value in C3A 2D monolayer (μM)
Paracetamol	8606	33826
Diclofenac	306	Non toxic
Trovafloxacin	319	440
Fialuridine	206	380

Table 2.1. Toxicological analysis of spheroids. *Spheroids were created from 1000 C3A cells by liquid-overlay technique, using 2D monolayer C3A cells as a comparison, and treated with 4 hepatotoxins. Cell viability was analysed IC_{50} values calculated. Data are represented as mean values (n=3).*